Cluster Analysis of Urban Ultrafine Particles Size Distributions

Agudelo-Castaned, Dayana Milena; Teixeira, Elba C.; Braga, Marcel; Alves Rolim, Silvia Beatriz; Silva, Luis F.O.; Beddows, David C.S.; Harrison, Roy; Querol, Xavier

DOI:
10.1016/j.apr.2018.06.006

Document Version
Peer reviewed version

Citation for published version (Harvard):
Agudelo-Castaned, DM, Teixeira, EC, Braga, M, Alves Rolim, SB, Silva, LFO, Beddows, DCS, Harrison, R & Querol, X 2019, 'Cluster Analysis of Urban Ultrafine Particles Size Distributions', *Atmospheric Pollution Research*, vol. 10, no. 1, pp. 45-52. https://doi.org/10.1016/j.apr.2018.06.006

Cluster Analysis of Urban Ultrafine Particles Size Distributions

Agudelo-Castaned, Dayana Milena; Teixeira, Elba C.; Braga, Marcel; Alves Rolim, Silvia Beatriz; Silva, Luis F.O.; Beddows, David C.S.; Harrison, Roy; Querol, Xavier

Cluster analysis of urban ultrafine particles size distributions

Dayana Milena Agudelo-Castañed[a]; Elba C. Teixeira[b,c,1]; Marcel Braga[c]; Silvia Beatriz Alves Rolim[a]; Luis F.O. Silva[d] ; David C.S. Beddows[e] ; Roy M. Harrison[e,f] and Xavier Querol[g]

[a]Department of Civil and Environmental Engineering, Universidad del Norte, Km 5 – Vía Puerto, Barranquilla, Atlántico, 081007, Colombia

[b]Research Department, Fundação Estadual de Proteção Ambiental Henrique Luís Roessler, Av. Borges de Medeiros, 261, Porto Alegre, RS, 90020–021, Brazil.

[c]Postgraduate Program in Remote Sensing and Meteorology, Geosciences Institute, Universidade Federal do Rio Grande do Sul, Av. Bento Gonçalves, 9500, Porto Alegre, RS, 91501–970, Brazil

[d]Civil and Environmental Department, Universidad De La Costa. Calle 58 #55–66, Barranquilla, Atlántico, 080002, Colombia

[e]National Centre for Atmospheric Science Division of Environmental Health & Risk Management School of Geography, Earth & Environmental Sciences, University of Birmingham, Edgbaston, Birmingham, B15 2TT, United Kingdom

[f]Department of Environmental Sciences/Center of Excellence in Environmental Studies, King Abdulaziz University, Jeddah, 21589, Saudi Arabia

[g]Institute for Environmental Assessment and Water Research (IDÆA-CSIC), C/ Jordi Girona 18-26, 08034 Barcelona, Spain

ABSTRACT

Measurements of particle size distribution was made in one location of an urban area in the period January-September/2015 in order to understand the sources and mechanisms influencing ultrafine particle (UFP) number concentrations ($PNC_{2.5-250}$) using a Scanning Mobility Particle Sizer Spectrometer (SMPS). k-means cluster analysis was applied to interpret the sources, temporal and spatial trends of UFP. Eight clusters were obtained. Main PSD patterns of each cluster, mean concentration of other air pollutants

[1] Corresponding author. Research Department, Fundação Estadual de Proteção Ambiental Henrique Luis Roessler, Rua Borges de Medeiros 261/9 Andar, 90020-021,Porto Alegre, RS, Brazil.E-mail address:ecalessoteixeira@gmail.com(E.C. Teixeira).

tracing specific sources and processes, and that of meteorological variables, as well as the hourly and seasonal frequencies of occurrence were used to support the interpretation of their origin. Thus, clusters were attributed to traffic rush hours, midday summer new particle formation, diurnal new particle formation and growth, growth of nucleated and other urban particles, urban background, regional and urban background and regional and urban background on cold nights. Many PSDs of the clusters were dominated by nucleation mode particles: midday nucleated fresh particles, photochemically induced (NPF); diurnal nucleation episodes (NPF2); growth of nucleated particles in nocturnal aging (GNPF). Origins of the clusters were related to local/regional sources (mostly traffic and biomass burning), atmospheric processes (photochemical formation and growth) and urban/regional background. Results clearly shows that traffic is a major UFP source in nucleation mode and occurred in higher concentrations in winter (08:00 to 12:00 h) during traffic rush hours, and at night. Photochemical nucleation occurred with a relatively low frequency but yielding very high PNC.

Keywords: Nanoparticles; Clusters analysis; Particle number concentration; particle size distribution, ultrafine particles.

1. Introduction

Atmospheric ultrafine particles (UFP, or particles <100 nm) can affect atmospheric chemistry, human health and climate (Atkinson et al., 2014; Kulmala et al., 2016a, 2004; among others). Therefore, a number of studies have reported the importance of studying, and some of them of minimizing concentrations, of atmospheric UFP (Horvath et al., 1996; Kulmala et al., 2004; Murr and Garza, 2009). The atmospheric

66 particle number concentration (PNC) is dominated by that of the UFP size range
67 (Cheung et al., 2013), and accordingly we will use in this paper the terms PNC and UFP
68 interchangeably. These UFP contribute to an increase in the health impact of aerosols
69 because their very fine size allows UFP to penetrate and deposit in the deepest parts of
70 the respiratory system, or even penetrate the pulmonary epithelium and olfactory nerve
71 (HEI, 2013, and papers therein) and reach the cardiovascular system and hence other
72 body organs.

73 The origin of UFP can be related to specific emission sources (mostly combustion
74 sources), such as road traffic, shipping, airports, industrial sources (Buonanno and
75 Morawska, 2015; Charron and Harrison, 2003; Cheung et al., 2013; Johnson et al.,
76 2014; Keuken et al., 2015a, 2015b), or newly produced within the atmosphere by
77 nucleation processes (Jamriska et al., 2008; Kumar et al., 2010; Morawska et al., 2008).
78 Thus, UFP may be of both primary and secondary origin.

79 In urban areas evidence suggest that road traffic is the main source of UFP in cities
80 (Dall'Osto et al., 2012; Kumar et al., 2014; Ma and Birmili, 2015; Morawska et al.,
81 2008; Pey et al., 2009; Salma et al., 2014) and these arise from primary UFP exhaust
82 emissions (Charron and Harrison, 2003; Shi et al., 2001; Shi and Harrison, 1999;
83 Uhrner et al., 2007), including those from new particle formation (NPF) from semi-
84 volatile phases which condense to create new UFP during dilution and cooling of the
85 exhaust emissions very close to the source point (Charron and Harrison, 2003; Kittelson
86 et al., 2006; Robinson et al., 2007). Some previous studies showed that the
87 airport/airliner is also one of the main UFP sources in cities. However, its affecting area
88 may be limited to rural-urban/near airport areas (Ren et al., 2016).

89 PSD of particles emitted from diesel vehicle engines fall mainly in the range of 20–130
90 nm, while for petrol these are in the 40-80 nm range (Morawska et al., 2008; Ristovski
91 et al., 2006). Brines et al., (2015) using a long time series of data on ambient PSD of

92 urban UFP found major modes in the 20–40 nm (traffic-related nucleated particles) and
93 another at 70–130 nm (soot particles) for periods of high 'fresh' traffic pollution from a
94 number of cities. In addition, they found to this freshly emitted traffic PSD, two other
95 traffic-related size distributions. One of them, with a minor 20–40 nm mode and a
96 dominant mode at 70–90 nm, interpreted as the result of growth (by condensation and
97 coagulation) during evening and night of the fresh traffic particles; and the second with
98 similar modes, but shifted to 10–20 nm and a main peak at 50–90 nm throughout the
99 day, with a peak during daytime. They attributed the shift to smaller sizes of the 20–40
100 nm peak of freshly emitted particles as due to particle evaporation.

101 On the other hand, photochemical NPF events are common in less polluted
102 environments. These new particles are formed from photochemical nucleation of H_2SO_4
103 and H_2SO_4-NH_3 followed by growth by condensation of the same gaseous species and
104 oxidation products of volatile organic compounds (VOCs) (Kulmala et al., 2016a,
105 2004). Thus, high insolation (favouring photochemical transformations), high wind
106 speed (favouring nucleation by decreasing the condensation sink when UFP are
107 dispersed), low relative humidity (favouring nucleation instead of condensation), and
108 available SO_2 (supplying H_2SO_4 for nucleation) may produce intensive NPF episodes
109 (Kulmala et al., 2016a, 2004; Kulmala and Kerminen, 2008), characterized by a marked
110 increase in PNC in the nucleation mode, and a subsequent particle growth yielding the
111 'banana like' nucleation bursts. Cheung et al. (2013) and Brines et al. (2015)
112 demonstrated that in the urban atmosphere most NPF events are not followed by a large
113 condensation/growth stage, but are only nucleation bursts, probably due to the delay of
114 nucleation due to the high particle concentrations in the morning traffic rush hours, and
115 the increase of the condensation sink by the afternoon traffic emissions. Thus the high
116 condensation sink caused by traffic emissions gives only a relatively short period for
117 nucleation in the middle of the day.

While at remote and low-pollution sites PSD can be similar over longer periods of time, excluding the nucleation and growth episodes, this is not generally the case at more polluted urban sites given the variations of emission fluxes and the influence of meteorology on these, (Wegner et al., 2012). Studies performed in Rochester, US showed that policy measures to abate primary particles and precursors and recession effects caused a clear decrease of UFP-PNC (in this case at a rate of -4.5%/year, Masiol et al., 2018). Thus, in spite of the complexity and multiple factors affecting PNC, policy measures might have a clear influence.

Studies on UFP, PSD and NPF have been conducted in different environments and numerous locations around the world, principally in temperate regions and developed countries (mostly Europe, Canada and US). Though, in developing countries such as Brazil, no studies have been done at urban/industrial regions. This subject requires research to get better information on the sources and aerosol processes governing concentrations and variability of UFP. This evaluation can be achieved by applying cluster analysis to long time series of measurements of PSDs (Beddows et al., 2009). This clustering technique classifies aerosol size spectra into a reduced number of categories or clusters that can be characterized considering their size peaks, temporal trends and meteorological and gaseous pollutants average values (Brines et al., 2015).

Thus, the aim of this study is to identify possible sources and aerosol processes related with the emission, formation and transformations of UFPs in the urban area of Porto Alegre (South Brazil). To this end, cluster analysis was applied to a long data set of PSDs. The interpretation of the origin of the PSDs of each cluster was supported by calculating the averaged concentrations of PNCs and other pollutants, as well as the means of meteorological parameters, and their frequency of occurrence at hourly and seasonal scales.

2. Study area

The study area is the city of Canoas, located in the Metropolitan Area of Porto Alegre (MAPA), in the central-eastern region of the state of Rio Grande do Sul, Southern Brazil. This area has its limits within 29°54′ to 29°20′ S and 51°17′ to 50°15′ W. The meteorological conditions have been described in previous studies (Teixeira et al., 2012).

According to Koppen's international system of climate classification, the climate type of the study area is a humid subtropical climate (Cfa) with well distributed rain over all the year. Due to its location, the area of study shows well-defined seasons and a climate strongly influenced by cold air masses migrating from the polar regions. The historical average rainfall is 1300-1400mm·yr-1 (INPE-CPTEC, 2012). The area of study is located in a subtropical, temperate climate with four well-defined seasons: summer (January-March), autumn (April-June), winter (July-September), and spring (October-December) with means temperature of 24.4 °C, 17.7 °C, 15.5 °C and 21.4 °C, respectively (Table S1). The wind direction shows marked seasonal variations. During summer and spring, the prevailing direction is E-SE, while in fall and winter, besides E-SE winds, winds from W and NW also occur. During the day, the wind reaches its lowest speed at dawn and early morning, with highest speeds in the late afternoon, between 17:00–18:00. The prevailing wind results from interactions of mesoscale phenomena, especially sea/land breezes (from the Atlantic Ocean and the Patos Lagoon) and valley/mountain breezes (from the nearby Serra Geral Mountains located to the north of the MAPA).

According to the Brazilian Institute of Geography and Statistics (IBGE, 2013), this region comprises an area of 9653 km^2, representing 3.76% of the total area of the state, and has a population of 4.12 million inhabitants, i.e., 37.7% of the total population of Rio Grande do Sul. The MAPA is the most urbanized area in Rio Grande do Sul, and it

also contains different types industries, coal power plants and significant influence of mobile sources as: BR-116 highway located 450 m East, Air Base located ≈3000 m East/Northeast; oil refinery REFAP located ≈ 6800 m - North/Northeast, steel mill GERDAU located ≈ 12700 m – North and the Petrochemical Complex at ≈ 21000 m-West/Northwest. In addition to the industrial emissions, it is estimated that the most significant contribution to the MAPA emission inventory of air pollutants is due to the large number of vehicles in circulation in the region, 1.96 million (DETRAN, 2013). In 2009, the distribution of the fleet by fuel type in MAPA was 69% gasoline, 16% gasoline motorcycles, 11% diesel, and 4% alcohol (Teixeira et al., 2011). Canoas is under a strong influence of road traffic emissions, with daily traffic congestion.

3. Material and methods

24-hour continuous sampling was carried out using a TSI Scanning Mobility Particle Sizer Spectrometer (SMPS) 3936NL88 for atmospheric particles with diameters from 2.5 to 250 nm and for PNC up to >1000000 #/cm^3. SMPS included a neutralizer before entering the Differential Mobility Analyzer. SMPS is a high resolution nanoparticle sizer that uses a electrostatic classifier. This method is based on the physical principle that the ability of a particle to traverse an electric field is related to particle size. This equipment operates in conjunction with a particle counter (CPC). CPC 3788 is a particle counter that uses water-based condensation technology. Particles that are too small to be scatter enough to be detected by conventional optics are grown to a larger size by condensation to be measured. Those equipment were calibrated by the manufacturer (TSI) using NIST traceable analytical tools. This calibration was valid during the time they were used in this research. Measurements of meteorological

196 variables (temperature, relative humidity, wind and solar radiation) and concentrations
197 of other pollutants (PM_{10}, NO, NO_2, O_3, SO_2) were carried out simultaneously to those
198 of the SMPS from January to September 2015. The SMPS and meteorological station
199 were located in the city of Canoas (Military Air Base), in the metropolitan area of Porto
200 Alegre, in the air quality monitoring station. This area has its limits within 29°54′ to
201 29°20′ S and 51°17′ to 50°15′ W. The monitoring station is located at 20 m.a.s.l. at the
202 following location: 29°55'50.0"S 51°10'56.5"W at 370 m from the highway (BR-116).
203

204 ## 4. Data analysis

205 Given the amount of data to be analyzed and the complexity of the study a statistical
206 analysis was applied to the SMPS data set using k-means cluster analysis that classifies
207 PSD spectra with the highest degree of similarity into the same category or cluster,
208 therefore reducing the number of spectra to interpret (Beddows et al., 2009). The cluster
209 analysis was performed using hourly averaged PSD data (39 size bins and 4760 h).
210 Cluster validation indices were used to choose the optimum number of spectra to divide
211 the data as described elsewhere (Beddows et al., 2009; Dall'Osto et al., 2013a). This is
212 solely a statistical analysis based on the clustering of the shape of the spectra. The use
213 of cluster analysis was justified in this research using a Cluster Tendency test, providing
214 a calculated Hopkins Index of 0.20 and implying the presence of structures in the form
215 of cluster in a dataset. The choice of k-means clustering was made from a selection of
216 the partitional cluster packages (Beddows et al., 2009). The k-means method aims to
217 minimize the sum of squared distances between all points and the cluster centre. K-
218 means clustering identifies homogeneous groups by minimizing the clustering error
219 defined as the sum of the squared Euclidean distances between each dataset point and
220 the corresponding cluster center. The complexity of the dataset is reduced allowing
221 characterization of the data according to the temporal and spatial trends of the clusters.

In order to choose the optimum number of clusters the Dunn-Index (DI) was used, which aims to identify dense and well-separated clusters. DI is defined as the ratio between the minimal intercluster distance to maximal intra-cluster distance. Since internal criteria seek clusters with high intra-cluster similarity and low inter-cluster similarity, algorithms that produce clusters with high DI are more desirable. In other words, for Dunn's index we wanted to find the clustering which maximizes this index. The Dunn-Index for the results of the k-means cluster analysis for different cluster numbers showed a clear maximum for 8 clusters, some of which belonged only to specific times of the day, specific mechanisms as well as specific seasons.

The interpretation of the origin of each cluster was based on the dominant size modes, their seasonal and hourly frequency of occurrence and the average values obtained for other air pollutants and meteorological variables for each cluster.

5. Results and discussion

5.1. Averaged particle number concentrations

PNC obtained in this study was compared with other researches done around the world (Table S2). Differences between these sites might be due to differences in experimental methods, meteorology, cut-off size for the PNC measurements, distance to emission sources, topographic settings, seasonal effects, among others (Kumar et al., 2014), but also to the vehicle fleet composition. PNC obtained in the present study was lower than Los Angeles (US), although higher than those reported in Europe studies. Lower concentrations of PNC in Brisbane are, probably, due to lower diesel fleet proportion and higher precipitation rates (Brines et al., 2015). Similar PNC values were observed in Latin America, i.e. Santiago de Chile (Kumar et al., 2014). Probably, the higher values obtained in Canoas (Brazil), compared with other cities, is due to the diverse

247 industries and mobile sources, thay may led to the high levels of SO_2 and UFP.
248 Especially, the presence of the emission sources of the oil refinery (REFAP) and the
249 heavy duty vehicle fleet (uses diesel), and the increasing SO_2 trend in the MAPA
250 (Landim et al., 2018). Highest UFP values (>5.0E+5) were presented during two winter
251 days (9/06/2015 and 10/08/2015) at 10:00 h local time in the 50-80 nm, typical of traffic
252 related particles, especially diesel-soot particles, as will be discussed further on.

253

254 **5.2 Clusters identification and interpretation**

255 The average PSD in d*N*/dlog(D_p) for each of the eight clusters is presented in Figure 1.
256 Statistical optimization was used for the cluster validation index to choose the optimum
257 number of spectra to divide the data (Beddows et al., 2009; Brines et al., 2014;
258 Dall'Osto et al., 2013a). Characteristics of each cluster and the associated sources are
259 summarised in Table 1. Each cluster is explained in the following sub-sections. These
260 data (Figure 1 and Table 1) supported with those of the mean value of traffic pollutants
261 and meteorological variables for the time periods of specific cluster occurrence allowed
262 the interpretation of their possible origin (Table 2).

263

264 **5.2.1. Traffic clusters**

265 *Cluster 1 – Fresh vehicle exhaust during traffic rush-hours (TR1)*

266 Cluster 1 is the most frequent cluster (16.8% of the total hourly PSD) with a nucleation
267 mode at 20 nm (reaching ~ 20000 #/cm^3, Figure 1). The diurnal profile is characterized
268 by an occurrence peak during traffic rush hours in the morning (09:00h local time -
269 UTC-3 in winter and UTC-2 in summer) and evening (20:00h - UTC-3 in winter and
270 UTC-2 in summer) (Figure 1), and the highest NO_2 concentrations (Table 2), thus
271 indicating a high influence of vehicle exhaust emissions (Brines et al., 2014; Dall'Osto

et al., 2013b). As discussed in the introductory section, Brines et al. (2015) found a major mode for the traffic cluster representing freshly emitted UFP in the 20–40 nm (traffic-related nucleated particles) and another at 70–130 nm (diesel soot particles) for a number of cities. Studies done in Brisbane, Australia, Toronto, Canada, and Los Angeles, US, with a much lower proportion of diesel vehicles in their respective car fleets the traffic clusters were characterized by modes at 14-20, 22-26 and 15-30 nm, respectively (Kim et al., 2002, Sabaliauskas et al., 2013, Brines et al., 2015).

As explained above, the diesel vehicles fleet distribution in the MAPA is 11%. In addition to the timing and intensity of traffic emissions, the morning peak of this cluster is favoured, too, by an undeveloped mixed boundary layer, so that all emissions are accumulated (Agudelo-Castañeda et al., 2013; Wang et al., 2010). There is a synergistic effect between three factors: wind speed, height of the mixing layer and vehicular traffic. Reduced PNCs at midday may be favoured by atmospheric dispersion processes due to an increase of the mixing layer height (MLH) and to higher wind speed (Charron and Harrison, 2003). Wind speed tends to increase from the afternoon (the sampling site is downstream from the prevailing wind), and decreases early in the evening. The MLH decreases abruptly in the late afternoon, due to the extinction of the solar radiation, initiating the formation of the nocturnal layer, which is more stable. Following this, there is an increase of the accumulation of PNC favoured by the evening traffic rush hour, the wind carrying vehicular emissions towards the sampling site and by the decrease of the MLH, the nocturnal boundary layer, more stable (Agudelo-Castañeda et al., 2013). In the morning there is an inverse phenomenon, despite the increase of the vehicular emissions (rush hour), the winds are weaker and of variable direction (affecting the transport of pollutants to the site of sampling). Moreover, the incidence of solar radiation increases the height of the mixing layer (beginning of the convective layer).

298

299 *Cluster 4 – Aged vehicle exhaust, morning traffic (TR2)*

300 Cluster 4 contributed with 13.7 % of total hourly PNDs, with moderate-high PNC (peak
301 of ~20 000) of a unimodal size distribution spectrum with a peak centered in the 20-30
302 nm range (slightly shifted towards coarser sizes than TR1). This cluster has a marked
303 maximum frequency of occurrence slightly delayed to the morning traffic rush hours.
304 The late afternoon traffic rush hour is less evident in terms of frequency of occurrence
305 of this cluster. Cluster 4 is associated with high levels of pollutants from vehicle exhaust
306 such as NO_x, NO and PM_{10} (Figure 1 and Table 2). Brines et al. (Brines et al., 2015)
307 reported the occurrence of clusters with coarser PSD representing the growth (aging) of
308 freshly emitted traffic UFP. Seasonal maxima are recorded for TR2 in May-July,
309 whereas for TR1 it is in July-September.

310 To support the interpretation of the traffic origin of these clusters we calculated the
311 frequency of occurrence of TR1 (Cluster 1) and TR2 (Cluster 4) for the weekend and
312 week days and we normalized the frequencies for the number of weekend and weekdays
313 with measurements. Results evidenced that frequencies were distributed similarly for
314 weekdays, while for weekend the frequency was reduced (Table S3).

315

316 **5.2.2. Background clusters**

317 *Cluster 8 Nocturnal urban background aerosols on cold nights (NRUB)*

318 Cluster 8 accounts for 10.4 % of the total hourly PSDs, with peak in the Aitken mode at
319 90 nm reaching around 18 000 #/cm^3 (Figure 1). This cluster is characterised by the
320 coarsest PSD, nocturnal higher frequency of occurrence, mostly in June and August
321 (winter), the lowest temperature, wind speed, insolation, precipitation and O_3
322 concentrations, as well as the highest PM_{10}, NO, NO_X and humidity (Table 2). UFP

323 concentration peaks were present at diameters of 50–200 nm. These cluster patterns
324 have been attributed mainly to regional background aerosols during nights and cold
325 days (Krecl et al., 2017; Salimi et al., 2014). Ammonium nitrate, and in general
326 secondary aerosols, formation is favoured at night in cold and high humidity periods,
327 with thermal inversions that favours also the increase of PM and UFP concentrations by
328 a decrease of the MLH and the prevalence of stagnant conditions. Since we did not
329 measure nitrate, the contribution of this specie to this cluster cannot be ensured.

330

331 *Cluster 2 – Regional-urban background particles – biomass burning (R-UB)*

332 Cluster 2 reached a frequency of occurrence of 11.3% of the total hourly PSDs, and
333 presented, again, a unimodal size distribution with a mode centered at 50-60 nm, in the
334 Aitken mode, with PNC (~ 15 000 #/cm^3). The diurnal pattern is associated with a
335 minimum during morning rush hours and late afternoon, and a frequency peak in the
336 late night. This cluster is characterized by a coarser mode than the 'fresh' traffic
337 emission cluster. Coagulation and condensation processes affecting traffic particulate
338 emissions lead to particle growth and to the shift to coarser modes. This cluster has a
339 very similar PSD to that of the urban background cluster reported by Brines et al.
340 (2015) for the city of Brisbane (60 nm and unimodal), with a similarly low proportion
341 of diesel vehicles in the urban fleet. Moreover, biomass burning is one of the largest
342 sources of accumulation mode particles globally (Kumar et al., 2013); consequently
343 these particles with a regional and local origin, may also influence urban background
344 UFPs of this cluster. This cluster is highly associated with NO_x and PM_{10}, confirming
345 that incomplete combustion of biomass also may produce both gaseous and particulate
346 air pollution (Table 2). The highest occurrence was observed in May-July and at night,
347 implying a low MLH so UFP accumulated (Agudelo-Castañeda et al., 2017). One of the

348 lowest wind speeds also points to nocturnal accumulation of urban background
349 particles.

350

351 *Cluster 7 - Urban background (UB)*

352 Cluster 7 accounted 11.9 % of the total hourly PSDs (Figure 1). This cluster shows a
353 bimodal size distribution, with a nucleation mode at 20 nm, and a broader Aitken mode
354 with peak at 70 nm (both reaching moderate concentrations ~8 000 #/cm^3). Aitken
355 nuclei mode (20-90 nm) refers to an overlapping fraction of the nucleation and
356 accumulation mode, that arise from the growth or coagulation of nucleation mode
357 particles as well as by production in high numbers by primary combustion sources such
358 as vehicles (Kulmala et al., 2004; Kumar et al., 2010).

359 This cluster is characterized by high concentrations of traffic and industrial pollutants
360 (Table 2) such as PM_{10} (35 µg/m^3), NO_x (36 µg/m^3) and SO_2 (5.2 µg/m^3) concentrations.
361 The relatively low PNC and the nocturnal higher frequency of occurrence, very similar
362 to the R-UB cluster, but with higher diurnal frequencies points also to urban
363 background UFPs occurring as a link between traffic particles and the coarser regional-
364 urban background clusters in such a way that it has a bi-modal PSD because the diurnal
365 PSD (from 10:00-12:00 h) still contains particles in the early stages of aging. Maxima
366 of occurrence are sporadically recorded in May and August.

367 MAPA region is characterized by different types of industries that influence air quality,
368 including several fixed sources. Sources include an oil refinery, steel mills, steelworks;
369 petrochemical Industrial Complex (Pole); and two thermoelectric plants: Thermoelectric
370 Plant of Charqueadas (TERMOCHAR) and of São Jerônimo (TERMOSJ). The
371 thermoelectric plants use coal and the steelworks fuel oil. PNC for 50-100 nm particles

372 (Table 2) are similar to cluster 8 (Regional and urban background in cold nights) and
373 cluster 2 (Regional and urban background).

374

375 **5.1.3. Clusters of nucleation**

376 *Cluster 5– Midday nucleated fresh particles, photochemically induced (NPF)*

377 Cluster 5 represents only 3.9 % of the total hourly PSD with peak concentrations in the
378 nucleation mode reaching ~80 000 #/cm^3. Cluster 5 showed the highest normalized
379 concentration at <5 nm (Figure 1). New particle formation by nucleation grew to reach
380 the instrument detection size limit before growing further and gradually shifting to
381 coarser fractions. This cluster occurred mainly at midday (Figure 1) in January (warm
382 season)and May (atypical events of warm days), and was associated with the highest
383 insolation, temperature, concentrations of O_3 and SO_2, wind velocity, and with the
384 lowest humidity and NO_2, NO_X and PM_{10} concentrations (Table 2). All these conditions
385 favour photochemical nucleation according to Kulmala et al., (Kulmala et al., 2016a,
386 2004), and were found similarly associated with urban PSD clusters attributed to
387 photochemical nucleation in a number of cities by Salimi et al. (2014), Shi et al. (2001),
388 Dall'Osto et al. (Dall'Osto et al., 2013a, 2012), and Brines et al. (2015, 2014), among
389 others. The diurnal profile showed a peak frequency of occurrence of the NPF cluster at
390 15:00 h local time (UTC-3 in winter and UTC-2 in summer), characteristic of high
391 insolation and low condensation sink (due to PM dilution) and a minimum during night,
392 when growth processes prevail (see R-UB and RB clusters). As described before,
393 photooxidation of SO_2 to H_2SO_4 is usually the cause of nucleation (Kulmala et al.,
394 2016b, 2004). The higher SO_2 levels associated with the NPF cluster are evidenced, and
395 this pollutant is attributed to diverse industrial plants being operating at MAPA.

396

Cluster 6 – Diurnal nucleation episodes (NPF2)

Cluster 6 (Figure 1) represented 18% of the hours of measurement data. Interestingly, this cluster showed a relationship with low concentrations of traffic generated primary pollutants (PM_{10}, NO_x) associated with high levels of radiation and wind speed. This cluster presented a unimodal size distribution with the position of the mode at around 15 nm likely due to the contribution of nucleation processes, for low PNC (~15000 #/cm^3). Further analysis showed a relationship with the highest precipitation value and wind speed (Table 2). It appears that several types of atmospheric processes lead to particle formation, a possible regional nucleation event. During such events the growth of nucleated particles continues throughout the day, as observed in the daily profile (Figure 1). Several studies have shown that such events can occur more or less uniformly in air masses that extend over distances of hundreds of kilometers, in outflows of mid-latitude convective storms (Kulmala et al., 2004). Moreover, wind has a strong influence on the particle number, such that a stronger wind speed could reduce twofold the total number counts of particles at diameters ranging from 30 to 450 nm, but had no effect on the small particles (11-30 nm) (Vu et al., 2015). This is likely to be due to the reduction in condensation sink due to the accumulation and coarse mode particles reflected in a low PM_{10} concentration.

Cluster 3 – Growth of nucleated particles in nocturnal aging (GNPF)

Cluster 3 represents 14% of the total number particle distribution (Figure 1), and showed a mode for particles with a diameter less than 20 nm with low number concentration (~8 000 #/cm^3). The difference with UB (CL7) is the large proportion of the nucleation mode UFP presented in CL3. The diurnal pattern of occurrence is not strongly marked but peaking at nocturnal and early morning hours. Its diurnal pattern of

occurrence and association with a low concentration of traffic generated primary pollutants (NO_x) indicated that it had non-traffic related sources. Given the nocturnal higher frequency, this cluster presents lower levels of wind speed and insolation than clusters 5 and 6 (Table 2). Consequently, this cluster was attributed mainly to the growth of nucleated particles newly formed particles from cluster 6 in nocturnal aging. Thus, the cluster proximity diagram analysis (Figure 2) shows that the NPF (clusters 5 and 6) are at one end of the diagram and inter-related because of the finest PSD and the diurnal occurrence. Also, cluster 3 is directly related with 6 and 4 because it contains particles from NPF2 and TR2 that undergo growth processes during aging, that at the end will yield to UB PSD (cluster 7), with a bi-modal PSD; this size and time connection is also evidenced with a direct relation between clusters 3 and 7.

Clusters 1 and 4 are associated with most of the clusters that represent UFP generated by traffic, whose impact on urban UFP accounts for these two PSDs dominating the frequency of occurrence in the study area. In the opposite side of the diagram is the background cluster 2 presenting large modal diameters, due to the fact that the spectrum of the cluster showed aged UFP. Background clusters (2, 7, 8) are associated with traffic (1 and 4), nucleation and growth (5, 6 and 3). It is interesting to note that cluster 1 and cluster 2 are associated. Also, cluster 7 and 8 are associated, too (Figure 2). This suggests that the sources/processes generating cluster 1 and cluster 7 (linking traffic and background PSDs) develop and contribute to generation of wholly background clusters (cluster 2 and 8).

5.3 Particle number concentrations on cold and warm days

Figure 3 show average PNCs for each size mode for warm and cold days. Average PNC show that particles in the nucleation mode (<10 nm) had a maximum value of ~17 000

447 #/cm^3 on warm days, the highest mean PNC being in summer. As explained before in
448 the results obtained for cluster 5, the increased nanoparticle concentration in the
449 nucleation mode may be due to photochemical nucleation which depends strongly on
450 the intensity of solar radiation. On the other hand, the mean PNC for cold days started
451 to increase up to 20 nm with a predominance of #/cm^3, in the Aitken mode. Probably,
452 lower temperatures promote nucleation processes and atmospheric lifetime may
453 increase, associated with increased traffic exhaust emissions (Ripamonti et al., 2013). In
454 the 10-20 nm range, other studies revealed that maximum particle concentrations
455 occurred for both cold and warm days (Morawska et al., 2008; Wehner and
456 Wiedensohler, 2003).

457 Figure 4 compares average hourly PNC for summer and winter. PNC revealed higher
458 levels in winter time, ranging from 20,245 to 21,945 #/cm^3, in the morning from 8:00 to
459 12:00 during the periods of higher vehicle flow, and at night starting at 18:00, in a range
460 of 21,281- 21,071 #/cm^3. This reflects the results discussed above, which for cluster 1 a
461 peak was observed during traffic rush hours in the morning and evening. This pattern
462 may be attributed to particles generated from vehicle exhaust emissions. In addition, on
463 cold days, increased nucleation of combustion exhaust emitted from motor vehicles may
464 occur particularly during morning rush hours, as stated before (Morawska et al., 2008).
465 These authors reported that on colder days the greater atmospheric stability (less
466 dispersion) and lower mixing layer height probably contribute to the increase in PNC.
467 Evidence suggests that average PNC was highest in cold days affected by traffic
468 emissions (Fujitani et al., 2012; Pirjola et al., 2006).

469 Several other studies have been cited on seasonal variations most of which reveal lower
470 concentration in summer and higher concentrations in winter (Wehner and
471 Wiedensohler, 2003; Wu et al., 2008). These authors reported, too, that particle
472 formation is enhanced in periods of lower temperature, from traffic exhaust, especially

473 during the rush hours and with higher temperatures from photochemical particle
474 formation, with levels ranging from 14,028 to 13,841 #/cm^3 between 12:00 and 15:00.

475

476 ## 6. Conclusion

477

478 The measurements of PSD were made in an urban area, MAPA-Brazil, in the period of
479 January 2015 to September 2015, employing a SMPS. K-means clustering analysis was
480 performed on the data collected, resulting in eight size distributions that described the
481 aerosol population.
482 The present technique has evaluated the particle size distributions in relation to
483 predominant sources; however variations in particles from a source or contributions
484 from multiple sources can make it difficult to identify the origin. Eight clusters and the
485 associated sources were identified in the urban area. A total of 30.5% of the
486 nanoparticles were contributed by two clusters representing the traffic emissions.
487 The nanoparticles associated with traffic emissions characterized in clusters TR1 and
488 TR2, showed a diurnal variation, with peaks during traffic rush hours in the morning,
489 and evening, characterized by a nucleation mode with a broader Aitken mode. This
490 study clearly showed that the traffic conditions influenced the particle measurements
491 and clearly identified the traffic sources. Background clusters showed similar
492 characteristics with UFPs associated with traffic particles and coarser modes. One of
493 them occurring during colder nights is probably associated to the condensation of
494 secondary species such as nitrate . These three clusters represent 33.6% the total of
495 particle count in the study.
496 The other three clusters observed were due to nucleation, and they represent 35.9% of
497 the nanoparticles. A nucleation mode characterized the nanoparticles in clusters
498 reflecting diurnal nucleation episodes (NPF2), growth of nucleated particles in

499 nocturnal aging (GNPF) and midday nucleated fresh particles (NPF). Photochemically
500 induced nucleation made a large contribution to nanoparticles in the nucleation mode
501 (<10nm). The nucleation clusters showed associations with different meteorological
502 variables and air pollutants. This may be explained mainly by aged particles formed
503 from growth of photochemically induced nucleation particles in the ambient air. The
504 nanoparticle concentration was affected by environmental conditions and depended
505 upon the emission type and meteorological conditions, showing seasonal variation. This
506 study showed the contribution of meteorological variables including wind speed and
507 especially precipitation that contributed to nucleation particle formation. The high SO_2
508 concentration associated with cluster NPF also associated with high solar radiation
509 contributed to nucleation events. Also, an increased PNC for particles <10 nm
510 (nucleation mode) was observed on warmer days due to phochemical nucleation.
511 These results are also important in terms of exposure assessment in public health
512 research. The highest particle number concentrations typically occur in urban areas, and
513 these nanoparticles also have the greatest effect on human health due to deposition of
514 particles in the respiratory system. Consequently, the health impact of nanoparticles
515 may vary from cluster to cluster due to the differing regional deposition of particles of
516 different sizes (Vu et al., 2015).
517

518 ## Acknowledgments

519

520 Authors thanks to CNPq for the financial support

521

522

523 ## References

524

525 Agudelo-Castañeda, D.M., Teixeira, E.C., Rolim, S.B. a., Pereira, F.N., Wiegand,
526 F., 2013. Measurement of particle number and related pollutant concentrations in an
527 urban area in South Brazil. Atmos. Environ. 70, 254–262.
528 https://doi.org/10.1016/j.atmosenv.2013.01.029

529 Agudelo-Castañeda, D.M., Teixeira, E.C., Schneider, I.L., Lara, S.R., Silva, L.F.O.,
530 2017. Exposure to polycyclic aromatic hydrocarbons in atmospheric PM 1.0 of
531 urban environments: Carcinogenic and mutagenic respiratory health risk by age
532 groups. Environ. Pollut. 224, 158–170. https://doi.org/10.1016/j.envpol.2017.01.075

533 Atkinson, R.W., Kang, S., Anderson, H.R., Mills, I.C., Walton, H.A., 2014.
534 Epidemiological time series studies of PM $_{2.5}$ and daily mortality and hospital
535 admissions: a systematic review and meta-analysis. Thorax 69, 660–665.
536 https://doi.org/10.1136/thoraxjnl-2013-204492

537 Brines, M., Dall'Osto, M., Beddows, D.C.S., Harrison, R.M., Gómez-Moreno, F.,
538 Núñez, L., Artíñano, B., Costabile, F., Gobbi, G.P., Salimi, F., Morawska, L.,
539 Sioutas, C., Querol, X., 2015. Traffic and nucleation events as main sources of
540 ultrafine particles in high-insolation developed world cities. Atmos. Chem. Phys. 15,
541 5929–5945. https://doi.org/10.5194/acp-15-5929-2015

542 Brines, M., Dall'Osto, M., Beddows, D.C.S., Harrison, R.M., Querol, X., 2014.
543 Simplifying aerosol size distributions modes simultaneously detected at four
544 monitoring sites during SAPUSS. Atmos. Chem. Phys. 14, 2973–2986.
545 https://doi.org/10.5194/acp-14-2973-2014

546 Buonanno, G., Morawska, L., 2015. Ultrafine particle emission of waste incinerators
547 and comparison to the exposure of urban citizens. Waste Manag. 37, 75–81.
548 https://doi.org/10.1016/j.wasman.2014.03.008

549 Chalupa, D.C., Morrow, P.E., Oberdörster, G., Utell, M.J., Frampton, M.W., 2004.

550 Ultrafine particle deposition in subjects with asthma. Environ. Health Perspect. 112,
551 879–882. https://doi.org/10.1289/ehp.6851

552 Charron, A., Harrison, R.M., 2003. Primary particle formation from vehicle
553 emissions during exhaust dilution in the roadside atmosphere. Atmos. Environ. 37,
554 4109–4119. https://doi.org/10.1016/S1352-2310(03)00510-7

555 Cheung, H.C., Chou, C.C.-K., Huang, W.-R., Tsai, C.-Y., 2013. Characterization of
556 ultrafine particle number concentration and new particle formation in an urban
557 environment of Taipei, Taiwan. Atmos. Chem. Phys. 13, 8935–8946.
558 https://doi.org/10.5194/acp-13-8935-2013

559 Dall'Osto, M., Beddows, D.C.S., Pey, J., Rodriguez, S., Alastuey, A., M. Harrison,
560 R., Querol, X., 2012. Urban aerosol size distributions over the Mediterranean city of
561 Barcelona, NE Spain. Atmos. Chem. Phys. 12, 10693–10707.
562 https://doi.org/10.5194/acp-12-10693-2012

563 Dall'Osto, M., Querol, X., Alastuey, A., Minguillon, M.C., Alier, M., Amato, F.,
564 Brines, M., Cusack, M., Grimalt, J.O., Karanasiou, A., Moreno, T., Pandolfi, M.,
565 Pey, J., Reche, C., Ripoll, A., Tauler, R., Van Drooge, B.L., Viana, M., Harrison,
566 R.M., Gietl, J., Beddows, D., Bloss, W., O'Dowd, C., Ceburnis, D., Martucci, G.,
567 Ng, N.L., Worsnop, D., Wenger, J., Mc Gillicuddy, E., Sodeau, J., Healy, R.,
568 Lucarelli, F., Nava, S., Jimenez, J.L., Gomez Moreno, F., Artinano, B., Prévôt,
569 A.S.H., Pfaffenberger, L., Frey, S., Wilsenack, F., Casabona, D., Jiménez-Guerrero,
570 P., Gross, D., Cots, N., 2013a. Presenting SAPUSS: Solving aerosol problem by
571 using synergistic strategies in Barcelona, Spain. Atmos. Chem. Phys. 13, 8991–
572 9019. https://doi.org/10.5194/acp-13-8991-2013

573 Dall'Osto, M., Querol, X., Amato, F., Karanasiou, A., Lucarelli, F., Nava, S.,
574 Calzolai, G., Chiari, M., 2013b. Hourly elemental concentrations in PM2.5 aerosols

575 sampled simultaneously at urban background and road site during SAPUSS –
576 diurnal variations and PMF receptor modelling. Atmos. Chem. Phys. 13, 4375–
577 4392. https://doi.org/10.5194/acp-13-4375-2013

578 DETRAN, 2013. Departamento Estadual de Trânsito de Rio Grande do Sul [WWW
579 Document].

580 Fujitani, Y., Kumar, P., Tamura, K., Fushimi, A., Hasegawa, S., Takahashi, K.,
581 Tanabe, K., Kobayashi, S., Hirano, S., 2012. Seasonal differences of the
582 atmospheric particle size distribution in a metropolitan area in Japan. Sci. Total
583 Environ. 437, 339–347. https://doi.org/10.1016/j.scitotenv.2012.07.085

584 HEI, 2013. Understanding the Health Effects of Ambient Ultrafine Particles. HEI
585 Review Panel on Ultrafine Particles. HEI Perspectives 3. Insights from HEI's
586 research, Boston, US, 108 pp.
587 https://www.healtheffects.org/system/files/Perspectives3.pdf

588 Horvath, H., Kasahara, M., Pesava, P., 1996. The size distribution and composition
589 of the atmospheric aerosol at a rural and nearby urban location. J. Aerosol Sci. 27,
590 417–435. https://doi.org/10.1016/0021-8502(95)00546-3

591 IBGE, 2013. Instituto Brasileiro de Geografia e Estatística [WWW Document].
592 https://www.ibge.gov.br/.

593 Jamriska, M., Morawska, L., Mergersen, K., 2008. The effect of temperature and
594 humidity on size segregated traffic exhaust particle emissions. Atmos. Environ. 42,
595 2369–2382. https://doi.org/10.1016/j.atmosenv.2007.12.038

596 Johnson, G.R., Juwono, A.M., Friend, A.J., Cheung, H.C., Stelcer, E., Cohen, D.,
597 Ayoko, G.A., Morawska, L., 2014. Relating urban airborne particle concentrations
598 to shipping using carbon based elemental emission ratios. Atmos. Environ. 95, 525–
599 536. https://doi.org/10.1016/j.atmosenv.2014.07.003

600 Keuken, M.P., Moerman, M., Zandveld, P., Henzing, J.S., 2015a. Total and size-
601 resolved particle number and black carbon concentrations near an industrial area.
602 Atmos. Environ. 122, 196–205. https://doi.org/10.1016/j.atmosenv.2015.09.047

603 Keuken, M.P., Moerman, M., Zandveld, P., Henzing, J.S., Hoek, G., 2015b. Total
604 and size-resolved particle number and black carbon concentrations in urban areas
605 near Schiphol airport (the Netherlands). Atmos. Environ. 104, 132–142.
606 https://doi.org/10.1016/j.atmosenv.2015.01.015

607 Kim, S., Shen, S., Sioutas, C., Zhu Y., Hinds W.C., 2002. Size Distribution and
608 Diurnal and Seasonal Trends of Ultrafine Particles in Source and Receptor Sites of
609 the Los Angeles Basin, Journal of the Air & Waste Management Association, 52:3,
610 297-307, DOI: 10.1080/10473289.2002.10470781

611 Kittelson, D.B., Watts, W.F., Johnson, J.P., 2006. On-road and laboratory evaluation
612 of combustion aerosols-Part1: Summary of diesel engine results. J. Aerosol Sci. 37,
613 913–930. https://doi.org/10.1016/j.jaerosci.2005.08.005

614 Krecl, P., Johansson, C., Targino, A.C., Ström, J., Burman, L., 2017. Trends in
615 black carbon and size-resolved particle number concentrations and vehicle emission
616 factors under real-world conditions. Atmos. Environ. 165, 155–168.
617 https://doi.org/10.1016/j.atmosenv.2017.06.036

618 Kulmala, M., Hõrrak, U., Manninen, H.E., Mirme, S., Noppel, M., Lehtipalo, K.,
619 Junninen, H., Vehkamäki, H., Kerminen, V.M., Noe, S.M., Tammet, H., 2016a. The
620 legacy of Finnish–Estonian air ion and aerosol workshops. Boreal Environ. Res. 21,
621 181–206.

622 Kulmala, M., Kerminen, V.M., 2008. On the formation and growth of atmospheric
623 nanoparticles. Atmos. Res. 90, 132–150.
624 https://doi.org/10.1016/j.atmosres.2008.01.005

625 Kulmala, M., Luoma, K., Virkkula, A., Petäjä, T., Paasonen, P., Kerminen, V.M.,
626 Nie, W., Qi, X., Shen, Y., Chi, X., Ding, A., 2016b. On the mode-segregated aerosol
627 particle number concentration load: Contributions of primary and secondary
628 particles in Hyytiälä and Nanjing. Boreal Environ. Res. 21, 319–331.

629 Kulmala, M., Vehkamäki, H., Petäjä, T., Dal Maso, M., Lauri, A., Kerminen, V.-M.,
630 Birmili, W., McMurry, P.H., 2004. Formation and growth rates of ultrafine
631 atmospheric particles: a review of observations. J. Aerosol Sci. 35, 143–176.
632 https://doi.org/10.1016/j.jaerosci.2003.10.003

633 Kumar, P., Morawska, L., Birmili, W., Paasonen, P., Hu, M., Kulmala, M.,
634 Harrison, R.M., Norford, L., Britter, R., 2014. Ultrafine particles in cities. Environ.
635 Int. 66, 1–10. https://doi.org/10.1016/j.envint.2014.01.013

636 Kumar, P., Pirjola, L., Ketzel, M., Harrison, R.M., 2013. Nanoparticle emissions
637 from 11 non-vehicle exhaust sources – A review. Atmos. Environ. 67, 252–277.
638 https://doi.org/10.1016/j.atmosenv.2012.11.011

639 Kumar, P., Robins, A., Vardoulakis, S., Britter, R., 2010. A review of the
640 characteristics of nanoparticles in the urban atmosphere and the prospects for
641 developing regulatory controls. Atmos. Environ. 44, 5035–5052.
642 https://doi.org/10.1016/j.atmosenv.2010.08.016

643 Landim, A.A., Teixeira, E.C., Agudelo-Castañeda, D., Schneider, I., Silva, L.F.O,
644 Wiegand, F., Kumar, P., Air Qual Atmos Health (2018).
645 https://doi.org/10.1007/s11869-018-0584-2

646 Ma, N., Birmili, W., 2015. Estimating the contribution of photochemical particle
647 formation to ultrafine particle number averages in an urban atmosphere. Sci. Total
648 Environ. 512–513, 154–166. https://doi.org/10.1016/j.scitotenv.2015.01.009

649 Masiol, M., Squizzato, S., Chalupa, D.C., Utell, M.J., Rich, D.Q., Hopke, P.K.,

650 2018. Long-term trends in submicron particle concentrations in a metropolitan area
651 of the northeastern United States. Science of The Total Environment, 633, 59-70.

652 Morawska, L., Ristovski, Z., Jayaratne, E.R., Keogh, D.U., Ling, X., 2008. Ambient
653 nano and ultrafine particles from motor vehicle emissions: Characteristics, ambient
654 processing and implications on human exposure. Atmos. Environ. 42, 8113–8138.
655 https://doi.org/10.1016/j.atmosenv.2008.07.050

656 Murr, L.E., Garza, K.M., 2009. Natural and anthropogenic environmental
657 nanoparticulates: Their microstructural characterization and respiratory health
658 implications. Atmos. Environ. 43, 2683–2692.
659 https://doi.org/10.1016/j.atmosenv.2009.03.002

660 Pey, J., Alastuey, A., Querol, X., Rodríguez, S., 2010. Monitoring of sources and
661 atmospheric processes controlling air quality in an urban Mediterranean
662 environment. Atmos. Environ. 44, 4879–4890.
663 https://doi.org/10.1016/j.atmosenv.2010.08.034

664 Pey, J., Querol, X., Alastuey, A., 2009. Variations of levels and composition of
665 PM10 and PM2.5 at an insular site in the Western Mediterranean. Atmos. Res. 94,
666 285–299. https://doi.org/10.1016/j.atmosres.2009.06.006

667 Pirjola, L., Paasonen, P., Pfeiffer, D., Hussein, T., Hämeri, K., Koskentalo, T.,
668 Virtanen, A., Rönkkö, T., Keskinen, J., Pakkanen, T.A., Hillamo, R.E., 2006.
669 Dispersion of particles and trace gases nearby a city highway: Mobile laboratory
670 measurements in Finland. Atmos. Environ. 40, 867–879.
671 https://doi.org/10.1016/j.atmosenv.2005.10.018

672 Ren, J.Liu, J., Li,F. Cao,X. Ren, S. Xu, B. A study of ambient fine particles at
673 Tianjin International Airport, China . Science of the total environment 556, 126-135.

674 Ripamonti, G., Järvi, L., Molgaard, B., Hussein, T., Nordbo, A., Hämeri, K., 2013.

675 The effect of local sources on aerosol particle number size distribution ,
676 concentrations and fluxes in Helsinki, Finland. Tellus B 1, 1–17.
677 https://doi.org/10.3402/tellusb.v65i0.19786

678 Ristovski, Z.D., Jayaratne, E.R., Lim, M., Ayoko, G.A., Morawska, L., 2006.
679 Influence of the Diesel Fuel Sulphur Content on the Nanoparticle Emissions From a
680 Fleet of City Buses. Int. Lab. 40, 1314–1320.

681 Robinson, A.L., Donahue, N.M., Shrivastava, M.K., Weitkamp, E.A., Sage, A.M.,
682 Grieshop, A.P., Lane, T.E., Pierce, J.R., Pandis, S.N., 2007. Rethinking Organic
683 Aerosols: Semivolatile Emissions and Photochemical Aging. Science (80-.). 315,
684 1259 LP-1262.

685 Sabaliauskas, K., Jeong, C-H., Yao, X., Yun-Seok, J., Evans, G.J., 2013. "Cluster
686 Analysis of Roadside Ultrafine Particle Size Distributions, Atmospheric
687 Environment, 70, 64-74.

688 Salimi, F., Ristovski, Z., Mazaheri, M., Laiman, R., Crilley, L.R., He, C., Clifford,
689 S., Morawska, L., 2014. Assessment and application of clustering techniques to
690 atmospheric particle number size distribution for the purpose of source
691 apportionment. Atmos. Chem. Phys. 14, 11883–11892. https://doi.org/10.5194/acp-
692 14-11883-2014

693 Salma, I., Borsós, T., Németh, Z., Weidinger, T., Aalto, P., Kulmala, M., 2014.
694 Comparative study of ultrafine atmospheric aerosol within a city. Atmos. Environ.
695 92, 154–161. https://doi.org/10.1016/j.atmosenv.2014.04.020

696 Shi, J.P., Evans, D.E., Khan, A.A., Harrison, R.M., 2001. Sources and concentration
697 of nanoparticles ((10 nm diameter) in the urban atmosphere 35, 1193–1202.

698 Shi, J.P., Harrison, R.M., 1999. Investigation of Ultrafine Particle Formation during
699 Diesel Exhaust Dilution. Environ. Sci. Technol. 33, 3730–3736.

https://doi.org/10.1021/es981187l

Teixeira, E., Oliveira, K., Meincke, L., Alam, K., 2011. Study of nitro-polycyclic aromatic hydrocarbons in fine and coarse atmospheric particles. Atmos. Res. 101, 631–639. https://doi.org/10.1016/j.atmosres.2011.04.010

Teixeira, E.C., Agudelo-Castañeda, D.M., Fachel, J.M.G., Leal, K.A., Garcia, K.D.O., Wiegand, F., 2012. Source identification and seasonal variation of polycyclic aromatic hydrocarbons associated with atmospheric fine and coarse particles in the Metropolitan Area of Porto Alegre, RS, Brazil. Atmos. Res. 118, 390–403. https://doi.org/10.1016/j.atmosres.2012.07.004

Uhrner, U., von Löwis, S., Vehkamäki, H., Wehner, B., Bräsel, S., Hermann, M., Stratmann, F., Kulmala, M., Wiedensohler, A., 2007. Dilution and aerosol dynamics within a diesel car exhaust plume-CFD simulations of on-road measurement conditions. Atmos. Environ. 41, 7440–7461. https://doi.org/10.1016/j.atmosenv.2007.05.057

Vu, T. V., Delgado-Saborit, J.M., Harrison, R.M., 2015. Review: Particle number size distributions from seven major sources and implications for source apportionment studies. Atmos. Environ. 122, 114–132. https://doi.org/10.1016/j.atmosenv.2015.09.027

Wang, F., Costabileb, F., Li, H., Fang, D., Alligrini, I., 2010. Measurements of ultrafine particle size distribution near Rome. Atmos. Res. 98, 69–77. https://doi.org/10.1016/j.atmosres.2010.05.010

Wegner, T., Hussein, T., Hämeri, K., Vesala, T., Kulmala, M., Weber, S., 2012. Properties of aerosol signature size distributions in the urban environment as derived by cluster analysis. Atmos. Environ. 61, 350–360. https://doi.org/10.1016/j.atmosenv.2012.07.048

725 Wehner, B., Wiedensohler, A., 2003. Long term measurements of submicrometer
726 urban aerosols: statistical analysis for correlations with meteorological conditions
727 and trace gases. Atmos. Chem. Phys. 3, 867–879. https://doi.org/10.5194/acp-3-867-
728 2003

729 Wu, Z., Hu, M., Lin, P., Liu, S., Wehner, B., Wiedensohler, A., 2008. Particle
730 number size distribution in the urban atmosphere of Beijing, China. Atmos. Environ.
731 42, 7967–7980. https://doi.org/10.1016/j.atmosenv.2008.06.022

732

LIST OF FIGURES

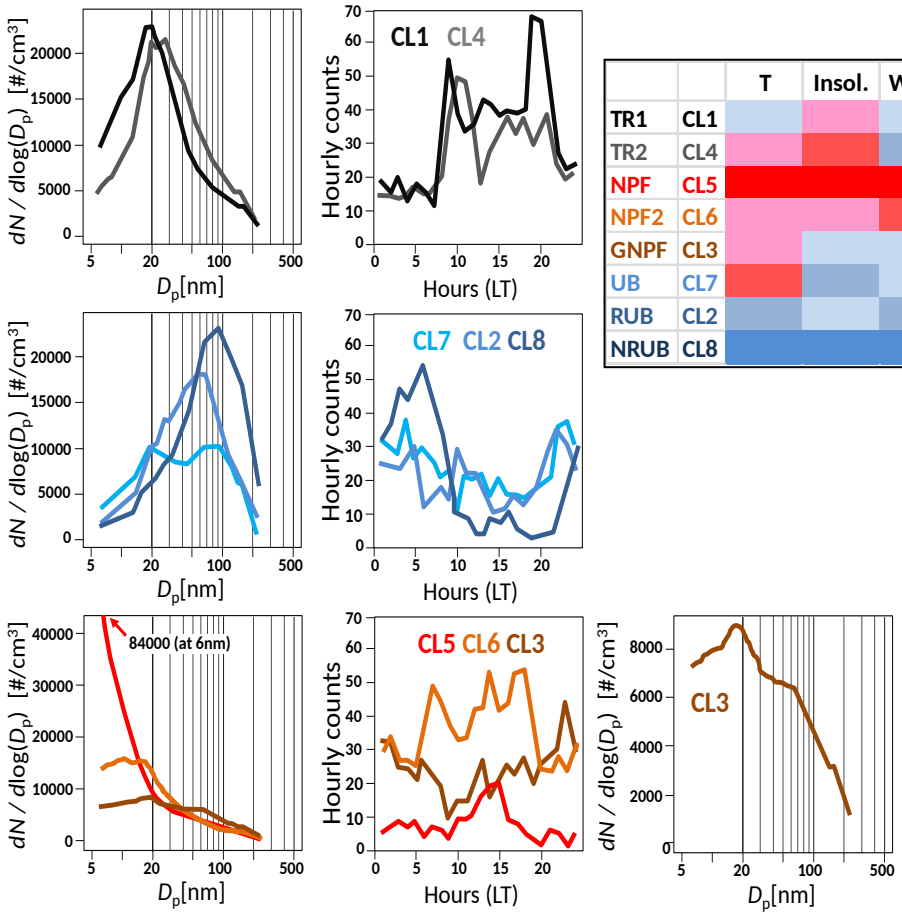

		T	Insol.	Wspd	O_3	SO_2	PSD	h/day	Season	RH	PM10	NO	NO_2	NO_X
TR1	CL1													
TR2	CL4													
NPF	CL5													
NPF2	CL6													
GNPF	CL3													
UB	CL7													
RUB	CL2													
NRUB	CL8													

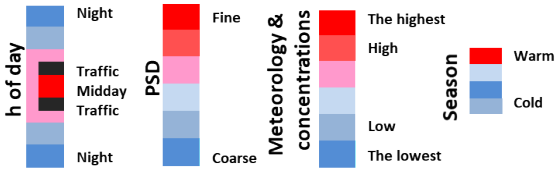

TR1 Traffic rush hours
TR2 Traffic morning rush hour
NPF Midday summer new particle (photochemical) formation
NPF2 Diurnal new particle (photochemical) formation and growth
GNPF Growth of nucleated and other urban particles
UB Urban background
RUB Regional and urban background
NRUB Regional and urban background during cold nights

Figure 1.

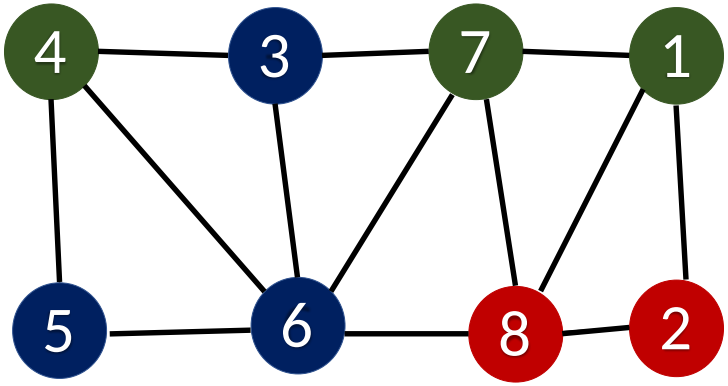

Figure 2.

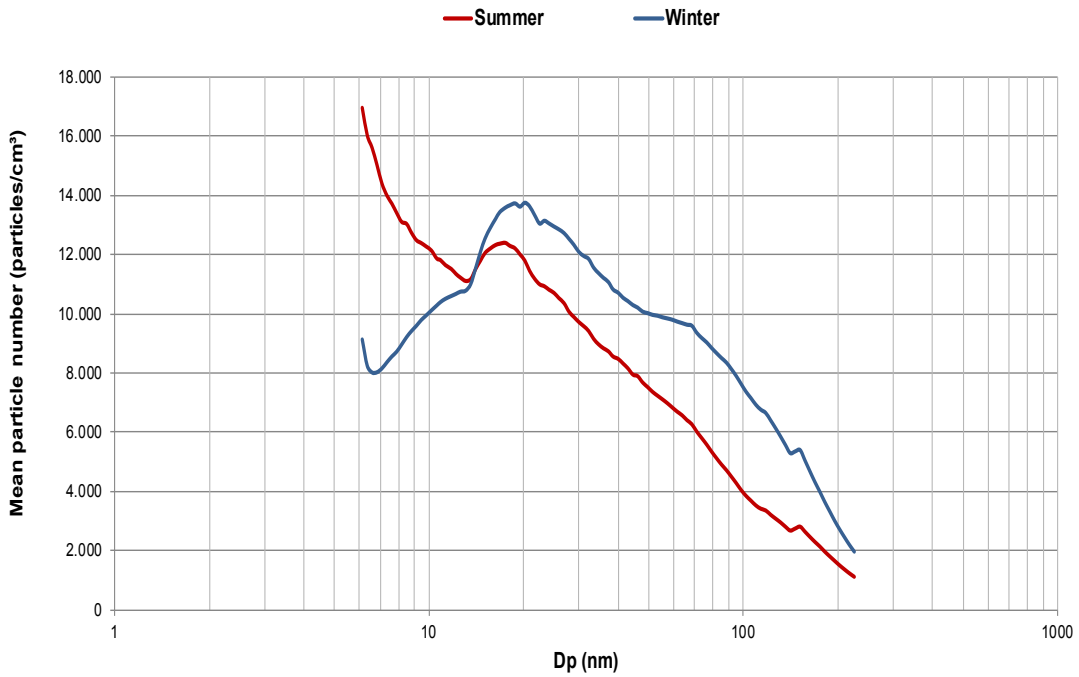
Summer
Winter
Mean particle number (particles/cm³)
18.000
16.000
14.000
12.000
10.000
8.000
6.000
4.000
2.000
0
1
10
100
1000
Dp (nm)

Figure 3

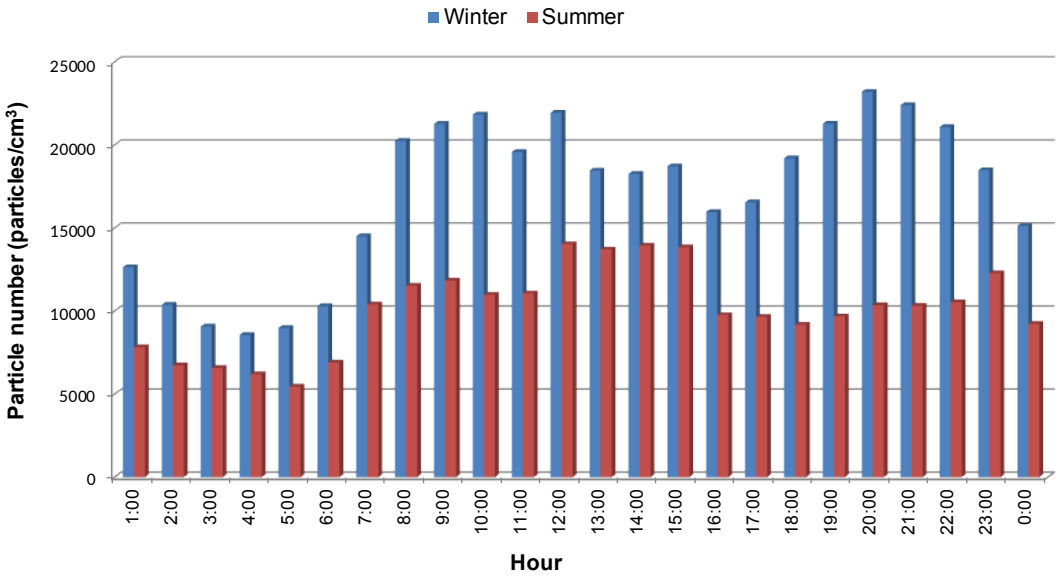
Winter
Summer
Particle number (particles/cm³)
25000
20000
15000
10000
5000
0
1:00
2:00
3:00
4:00
5:00
6:00
7:00
8:00
9:00
10:00
11:00
12:00
13:00
14:00
15:00
16:00
17:00
18:00
19:00
20:00
21:00
22:00
23:00
0:00
Hour

.

Figure 4.

LIST OF TABLES

Table 1.

Cluster number	Contribution to hours of PNC measurements	Source
1	16.8%	Fresh vehicle exhaust during traffic rush hours
2	11.3%	Regional and urban background
3	14%	Growth of nucleated and other urban particles
4	13.7%	Traffic morning rush hour
5	3.9%	Midday summer new particle (photochemical) formation
6	18%	Diurnal new particle (photochemical) formation and growth
7	11.9%	Urban background
8	10.4%	Regional and urban background in cold nights

Table 2.

	Cluster 1	Cluster 2	Cluster 3	Cluster4	Cluster 5	Cluster 6	Cluster 7	Cluster 8
PM_{10} . $ug \cdot m^{-3}$	19	34	25	26	16	17	35	57
NO . $ug \cdot m^{-3}$	12	24	13	24	10	9	18	39
NO_x . $ug \cdot m^{-3}$	34	44	28	44	22	24	36	57
NO_2 . $ug \cdot m^{-3}$	22	20	16	20	12	16	18	18
O_3 . $ug \cdot m^{-3}$	13	10	17	11	27	20	13	8
SO_2 . $ug \cdot m^{-3}$	5.1	4.8	4.7	4.3	6.2	4.12	5.2	4.2
Humidity. %	80	81	80	76	71	80	78	85
Wind speed. $m \cdot s^{-1}$	1.4	0.9	1.4	1.0	4	4	1.2	0.6
Solar radiation. $W \cdot m^{-2}$	557	414	401	665	1046	583	388	151
Temperature. °C	18	18	20	20	21	19	20	17
Precipitation. mm	0.30	0.13	0.30	0.18	0.19	0.37	0.11	0.07
total PNC	1.1E+04	9.9E+03	6.5E+03	1.1E+04	1.1E+04	7.9E+03	7.5E+03	8.4E+03
PNC<50nm	1.5E+04	9.2E+03	8.1E+03	1.5E+04	1.8E+04	1.2E+04	8.9E+03	5.0E+03
PNC50-100nm	6.2E+03	1.6E+04	6.0E+03	1.2E+04	3.8E+03	2.8E+03	1.1E+04	1.7E+04
PNC>100nm	2.7E+03	6.8E+03	3.0E+03	5.1E+03	1.6E+03	1.3E+03	7.5E+03	1.2E+04

SUPPLEMENTARY MATERIAL

Cluster analysis of urban ultrafine particles size distributions

Dayana Milena Agudelo-Castañed[a]; Elba C. Teixeira[b.c.1]; Marcel Braga[c]; Silvia Beatriz Alves Rolim[a]; Luis F.O. Silva[d] ; David C.S. Beddows[e] ; Roy M. Harrison[e.f] and Xavier Querol[g]

[a]Department of Civil and Environmental Engineering. Universidad del Norte. Km 5 – Vía Puerto. Barranquilla. Atlántico. 081007. Colombia

[b]Research Department. Fundação Estadual de Proteção Ambiental Henrique Luís Roessler. Av. Borges de Medeiros. 261. Porto Alegre. RS. 90020–021. Brazil.

[c]Postgraduate Program in Remote Sensing and Meteorology. Geosciences Institute. Universidade Federal do Rio Grande do Sul. Av. Bento Gonçalves. 9500. Porto Alegre. RS. 91501–970. Brazil

[d]Civil and Environmental Department. Universidad De La Costa. Calle 58 #55–66. Barranquilla. Atlántico. 080002. Colombia

[e]National Centre for Atmospheric Science Division of Environmental Health & Risk Management School of Geography. Earth & Environmental Sciences. University of Birmingham. Edgbaston. Birmingham. B15 2TT. United Kingdom
[f]Department of Environmental Sciences/Center of Excellence in Environmental Studies. King Abdulaziz University. Jeddah. 21589. Saudi Arabia
[g]Institute for Environmental Assessment and Water Research (IDÆA-CSIC). C/ Jordi Girona 18-26. 08034 Barcelona. Spain

1 Corresponding author. Research Department, Fundação Estadual de Proteção Ambiental Henrique Luis Roessler, Rua Borges de Medeiros 261/9 Andar, 90020-021,Porto Alegre, RS, Brazil.E-mail address:ecalessoteixeira@gmail.com(E.C. Teixeira).

FIGURES

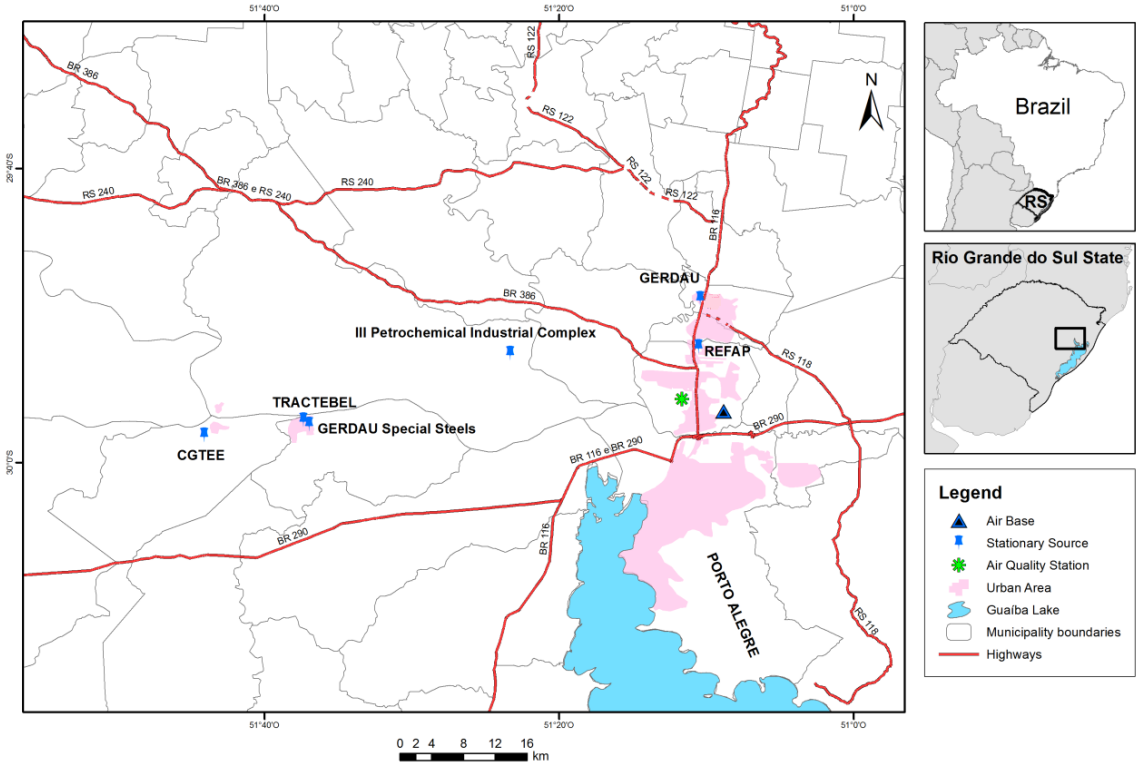

Figure S1: sampling site location.

TABLES

Table S1. Average meteorological conditions for the study period

	T (°)	H (%)	WS (m/s)	R (W/m^2)	PRP
Warm	24.1	77.6	3.4	210.5	389.2
Cold	17.6	78.5	2.9	113.3	926.4

T: averaged air temperature; H: averaged air humidity; WS: averaged wind speed; R: averaged global solar irradiance; PRP: accumulated precipitation.

Source: Salgado Filho Airport (T. H. WS) and Porto Alegre Meteorological Station (R. PRP).

Table S2. Comparison of ultrafine particle (UFP) number concentrations, in this study and different areas reported around the world.

	PNC (#/cm^3)	Sampling period	SMPS size range	Reference
Canoas	9000±7500	January- September /2015	2.5 - 250 nm	This study
Barcelona (Spain)	7500±5000	July 2012-August 2013	11.3– 358.7 nm	Brines et al., (2015)
Madrid (Spain)	7000±8000	January 2007- December 2008	17.5– 572.9 nm	Brines et al., (2015)
Brisbane (Australia)	6000±7000	January 2009- December 2009	10.2-101.8 nm	Brines et al., (2015)
Rome (Italy)	5000±3000	September 2007- May 2009	15.1– 224.7 nm	Brines et al., (2015)
Los Angeles (USA)	12000±7000	September 2009- December 2009	15.7-371.8 nm	Brines et al., (2015)
Santiago (Chile)	8020	2006	10-700 nm	Kumar et al., (2014)

Adapted from Brines et al., (2015) and Kumar et al. (2014)

Table S3. Average frequency distribution for weekdays and weekends by cluster

	TR1	R-UB	GNPF	TR2	NPF	NPF2	UB	NRUB
Monday	17.6%	8.3%	16.7%	13.9%	5.4%	19.0%	11.0%	8.1%
Tuesday	17.3%	9.6%	15.2%	13.5%	5.4%	20.8%	12.1%	7.4%
Wednesday	22.1%	10.0%	13.5%	13.3%	3.7%	18.1%	12.3%	9.0%
Thursday	20.7%	7.2%	13.5%	16.8%	5.1%	27.9%	9.0%	3.4%
Friday	19.9%	15.0%	12.6%	18.8%	3.2%	16.1%	11.9%	8.0%
Saturday	13.2%	17.3%	13.6%	14.5%	3.2%	11.2%	14.5%	17.5%
Sunday	11.6%	15.0%	15.0%	9.2%	3.2%	9.3%	16.1%	22.4%